Mineralogy and Petrology (1990) 42: 287–306

Mineralogy
and
Petrology

Platinum-Group Minerals from the Durance River Alluvium, France

Z. Johan[1], M. Ohnenstetter[1], W. Fischer[2], and J. Amossé[2]

[1] GIS BRGM-CNRS, Centre de Recherches sur la Synthèse et la Chimie des Minéraux Orléans, France, [2] Institut Dolomieu, Grenoble, France

With 4 Figures and 2 Plates

Received September 26, 1989;
accepted December 18, 1989

Summary

Platinum-group minerals were discovered, during gold recovery, in the Durance river alluvium, near Peyrolles (Bouches-du-Rhône). The PGM grains (average size 130 microns) are strongly flattened (average thickness 64 microns). The PGM concentrate consists primarily of (Pt, Fe) alloys (92%), (Os, Ir, Ru) alloys (3.5%), and native gold and (Au, Cu, Ag) alloys (4.5%). The following minerals were observed: isoferroplatinum, ferroan platinum, native osmium, native iridium, iridosmine, rutheniridosmine, osmiridium, ruthenian osmium, osmian ruthenium, cuprorhodsite, guanglinite, shandite, tetrauricupride, native gold, bornite, heazlewoodite, $(Pt, Pd)_2Cu_3$, Pt(Cu, Au), (Ni, Pt)Sn, $(Cu, Fe)_{1-x}(Pd, Rh, Pt)_{2+x}S_2$, $(Pt, Pd)_{4-x}Cu_2As_{1-x}$. Isoferroplatinum contains numerous inclusions of alloys, sulphides, arsenides, Pd-tellurides, and partly devitrified silicate-glass droplets. Most of the non-silicate inclusions also exhibit a drop-like shape indicating their original entrapment in a liquid state.

Cuprorhodsite crystals (up to 20 microns) are associated with bornite included in Pt_3Fe. Rarely, Pd- and Cu-sulphides, and Pd-tellurides appear in this association. Complex droplet-like arsenide inclusions in isoferroplatinum are composed of Pt-bearing guanglinite and $(Pt, Pd)_{4+x}Cu_2As_{1-x}$. Native iridium shows exsolutions of Ir-bearing isoferroplatinum and $(Pt, Pd)_2Cu_3$. In places, concentrations of Sn (up to 3 wt.%) were observed in (Au, Cu) alloys. Shandite and (Ni, Pt)Sn inclusions occur in (Au, Cu, Ag) alloys. Silicate-glass inclusions are TiO_2-poor and occasionally K-rich (plotting in the shoshonitic field). Taking into account mineralogical and chemical pecularities of the PGM association occurring in the studied concentrate, it seems highly probable that its primary source should be an Alaskan-type intrusion.

Zusammenfassung

Platingruppen Minerale aus dem Alluvium der Durance, Frankreich

Minerale der Platingruppe wurden im Zuge von Goldgewinnung im Alluvium der Durance in der Nähe von Peyrolles (Bouches-du-Rhône) entdeckt. Die PGM Körner (durchschnittliche Korngröße 130 μm) sind flach gepreßt (durchschnittliche Dicke 64 μm). Die PGM Konzentrate bestehen vorwiegend aus (Pt, Fe) Legierungen (92%); (Os, Ir, Ru) Legierungen (3,5%), sowie gediegen Gold und (Au, Cu, Ag) Legierungen (4,5%). Folgende Minerale wurden beobachtet:

Isoferro-Platin, Fe-Platin, gediegen Osmium, gediegen Iridium, Iridosmium, Rutheniridosmium, Osmiridium, Ru-Osmium, Os-Ruthenium, Cuprorhodsit, Guanglinit, Shandit, Tetrauricuprit, gediegen Gold, Bornit, Heazlewoodit, $(Pt, Pd)_2Cu_3$, Pt(Cu, Au), (Ni, Pt)Sn, $(Cu, Fe)_{1-x}(Pd, Rh, Pt)_{2+x}S_2$, $(Pt, Pd)_{4+x}.Cu_2As_{1-x}$.

Isoferro-Platin enthält zahlreiche Einschlüsse von Legierungen, Sulfiden, Arseniden, Pd-Telluriden und teilweise devitrifizierte Silikatglaströpfchen. Die meisten nichtsilikatischen Einschlüsse sind ebenfalls tröpfchenförmig. Dies weist darauf hin, daß sie in flüssigem Zustand eingeschlossen wurden.

Cuprorhodsitkristalle (bis zu 20 μm) sind gemeinsam mit Bornit in Pt_3Fe eingeschlossen. Selten sind Pd- und Cu-Sulfide, sowie Pd-Telluride mit diesen vergesellschaftet. Bei den komplexen tröpfchenförmigen Arsenideinschlüssen im Isoferro-Platin handelt es sich um Pt-führenden Guanglinit und $(Pt, Pd)_{4+x}Cu_2As_{1-x}$. Gediegen Iridium zeigt Entmischung von Ir-führendem Isoferro-Platin und $(Pt, Pd)_2Cu_3$. Stellenweise wurden Konzentrationen von Sn (bis zu 3%) in den (Au, Cu) Legierungen beobachtet. Shandit und (Ni, Pt)Sn Einschlüsse kommen in (Au, Cu, Ag) Legierungen vor. Silikatische Glaseinschlüsse sind TiO_2-arm und manchmal K-reich (im Shoshonitfeld liegend).

Auf Grund der mineralogischen und chemischen Eigenheiten der untersuchten PGM-Konzentrate ist eine Intrusion des Alaska-Typs als primäre Quelle sehr wahrscheinlich.

Introduction

Platinum concentrations were reported from various sedimentary units and mineralizations in the French Alps by *Gueymard* (1853). However, due to imperfect analytical techniques available in the 19th century, these results remained doubtful, and were never confirmed. However, since then *Fischer* et al. (1988) described isoferroplatinum from heavy-mineral separates collected during gold recovery in two sandpits working the Durance river alluvium near Peyrolles and at Pont de Rognonas (Bouches-du-Rhône). This is the first, well established, platinum occurrence in France.

In order to determine the possible primary sources of platinum discovered in the Durance river alluvium, a detailed mineralogical study of concentrate from Peyrolles has been undertaken. The concentrate was obtained by separation of heavy, fine-grained, minerals on rugs and by subsequent repeated panning. It must be stressed that most of the native gold present in these concentrates was previously dissolved by amalgamation. This prevented collection of data on relative proportions of native gold and platinum-group minerals (PGM) in the concentrate.

Mineralogy

The study of polished sections revealed a strong predominance of (Pt, Fe) alloys. The concentrate is composed of: 92% (Pt, Fe) alloys, 4.5% gold and (Au, Cu, Ag) alloys, and 3.5% (Os, Ir, Ru) alloys (percentage based on 200 grains). (Pt, Fe) alloys form discoidal particles described in detail by *Fischer* et al. (1988), whose average dimensions are 130 × 64 microns (180 measured grains). Statistics give a narrow range (0.064 mm; $\sigma = 0.031$) for the thickness of these particles. The size of (Os, Ir, Ru)

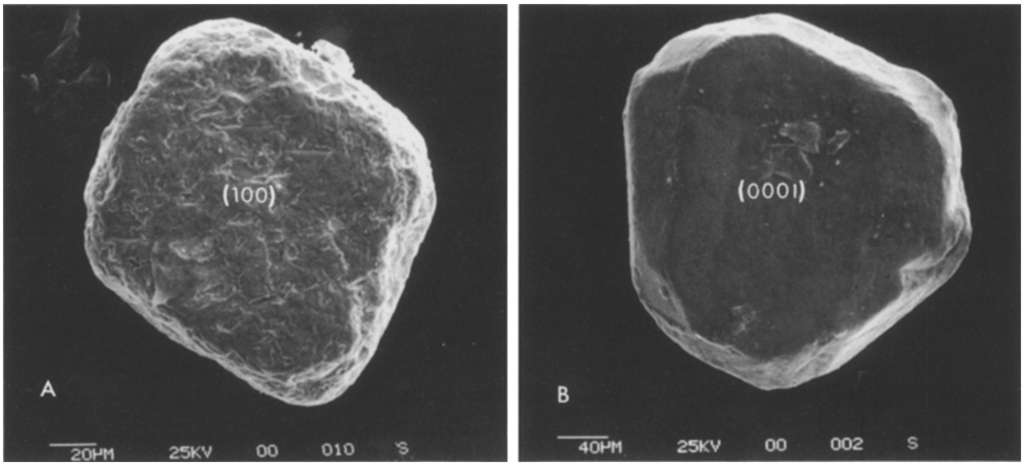

Fig. 1. Morphology of platinum minerals from the Peyrolles (Bouches-du-Rhône) concentrate. A) Crystal of (Pt, Fe) alloy with (100) crystal faces. SEM. B) Hexagonal crystal of (Os, Ir) alloy with (0001) and prismatic crystal faces. SEM

alloys is of the same order as that indicated for (Pt, Fe) alloys. The shape of native gold and Au-bearing alloys is much more irregular and indented. When examined by scanning electron microscopy (SEM), some PGM grains still exhibit their primordial crystal forms. Thus, (100) faces have been observed on (Pt, Fe) crystals (Fig. 1A), as well as (0001) and (10$\bar{1}$0) forms on iridosmine crystals (Fig. 1B). In view of the amount of wear observed on (Os, Ir, Ru) alloys and their hardness, a long transportation from the source area must be envisaged.

The following metallic mineral phases have been determined in the Peyrolles concentrate: isoferroplatinum, ferroan platinum, native osmium, native iridium, iridosmine, rutheniridosmine, osmiridium, ruthenian osmium, osmian ruthenium, cuprorhodsite, guanglinite, shandite, tetrauricupride, native gold, bornite, heazlewoodite, Pt(Au, Cu), $(\mathrm{Pt, Pd})_2\mathrm{Cu}_3$, (Ni, Pt)Sn, $(\mathrm{Cu, Fe})_{1-x}(\mathrm{Pd, Rh, Pt})_{2+x}\mathrm{S}_2$, $(\mathrm{Pt, Pd})_{4+x}\mathrm{Cu}_2\mathrm{As}_{1-x}$.

Microprobe analyses were carried out on the CAMEBAX microprobe (BRGM-CNRS microprobe laboratory in Orléans, *C. Gilles* and *D. Ohnenstetter*, analysts). Analytical conditions for PGM analysis: 25 kV accelerating voltage; analytical lines: RuLα, PtLα, FeKβ, RhLα, OsLβ, CuKα, PdLβ, IrLα, NiKα, SKα, AuLα, AgLα, AsLβ, SbLα, SnLα, PbMα; standards: pure Ru, Pt, Fe, Rh, Os, Cu, Pd, Ir, Ni, Au, Ag metals, FeS_2 (for S), $\mathrm{Sb}_2\mathrm{S}_3$ (for Sb), GaAs (for As), SnO_2 (for Sn), PbS (for Pb). The analytical data were corrected using the ZAF correction program. Additional corrections were made for Os–Au and Ir–Cu line interferences.

Platinum-Iron Alloys

Platinum-iron alloys and native iridium are the only PGM which contain inclusions or exsolutions of other mineral phases. In particular, they bear common minute inclusions of bornite associated with platinum-group element (PGE) sulphides and arsenides, as well as with silicate-glass inclusions described below. Microprobe study did not reveal any zoning. Selected microprobe analyses, given in Table 1, show however a large variation of Fe concentration which extends from approximately

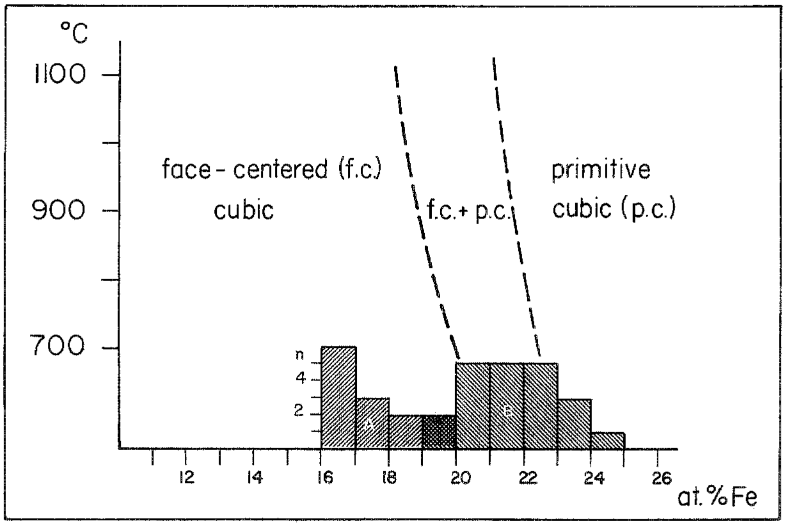

Fig. 2. Frequency distribution of Fe (at.%) in (Pt, Fe) alloys, schematically projected onto experimental data of *Cabri* and *Feather* (1975)

Table 1

	(Pt,Fe) ALLOYS				
	1	2	3	4	5
Ir	0.74	0.53	0.74	2.08	0.26
Ru	0.13	-	-	-	0.07
Rh	1.04	1.44	1.24	1.75	0.96
Pt	91.50	90.54	88.63	86.47	89.60
Pd	0.55	1.11	0.77	-	0.32
Fe	5.41	5.50	7.52	7.63	8.30
Ni	0.13	-	-	-	-
Cu	0.49	0.59	1.34	1.60	0.74
S	0.16	-	0.04	-	-
Total	100.15	99.71	100.28	99.53	100.25
Ir*	0.006	0.004	0.006	0.017	0.002
Ru	0.002	-	-	-	0.001
Rh	0.017	0.023	0.019	0.027	0.015
Pt	0.780	0.775	0.716	0.700	0.724
Pd	0.008	0.017	0.011	-	0.005
Fe	0.161	0.164	0.212	0.216	0.234
Ni	0.004	-	-	-	-
Cu	0.013	0.015	0.033	0.040	0.018
S	0.008	-	0.002	-	-

	NATIVE Au AND (Au,Cu) ALLOYS				
	1	2	3	4	5
Au	95.64	87.82	72.71	69.52	72.41
Ag	3.94	6.28	12.49	8.05	10.63
Cu	0.07	3.66	13.75	18.82	13.28
Ni	-	0.32	0.87	1.95	-
Fe	-	0.30	0.08	0.64	0.10
Sn	-	0.72	0.06	-	3.03
Pt	0.32	-	-	-	-
Pb	0.11	0.21	0.08	0.27	-
Total	100.08	99.31	100.04	99.25	99.45
Au*	0.924	0.769	0.514	0.458	0.523
Ag	0.070	0.100	0.161	0.097	0.140
Cu	0.002	0.100	0.301	0.385	0.298
Ni	-	0.010	0.021	0.043	-
Fe	-	0.009	0.002	0.015	0.003
Sn	-	0.010	0.001	-	0.036
Pt	0.003	-	-	-	-
Pb	0.001	0.002	-	0.002	-

*number of atoms calculated for the total of 1 per formula unit

16 to 24 at.%. Statistically, the chemical composition of (Pt, Fe) alloys exhibits a bimodal distribution with maxima at 16.5 (A) and 21.5 (B) at.% Fe (Fig. 2). Population A corresponds to grains devoid of inclusions whereas population B is characteristic of (Pt, Fe) alloys containing inclusions of bornite and cuprorhodsite.

Using the experimental data of *Cabri* and *Feather* (1975), it seems that population A is essentially composed of disordered (Pt, Fe) alloys (ferroan platinum), whilst the alloys belonging to population B are, at least partly, ordered (Fig. 2), corresponding to Pt_3Fe–isoferroplatinum (*Fischer* et al., 1988).

There is no evidence of any correlation between iron concentration and minor elements (Table 1). Rhodium, iridium, palladium and copper are consistently present, unlike osmium which is systematically absent. (Pt, Fe) alloys from the Durance river concentrate resemble isoferroplatinum and ferroan platinum from Papua-New Guinea (*Harris*, 1974) and Yubdo-Birbir in Ethiopia (*Cabri* et al., 1981). The chemical formulae of alloys belonging to population B range from $(Pt_{2.80}Rh_{0.11}Ir_{0.07})_{2.98} \cdot (Fe_{0.86}Cu_{0.16})_{1.02}$ to $(Pt_{2.96}Rh_{0.08}Pd_{0.04}Ir_{0.02})_{3.01}(Fe_{0.85}Cu_{0.13}S_{0.01})_{0.99}$. They show only minor deviation from the ideal formula Pt_3Fe.

(*Os, Ir, Ru*) *Alloys and Native Iridium*

(Os, Ir, Ru) alloys are characteristically devoid of inclusions, occurring as monocrystalline grains of approximately the same size as (Pt, Fe) alloys. Only one inclusion of native osmium was observed in Pt_3Fe (Plate 1-A; Table 2, analysis 4). Furthermore, iridium-rich alloys and native iridium exhibit exsolutions of Pt-, Cu-, and Fe-bearing phases (Plate 1-B, C, D). Microprobe analyses (Table 2) show a wide variation in chemical composition, but there is no evidence of any zoning observed elsewhere (*Cabri* and *Harris*, 1975). Using the nomenclature proposed by *Harris* and *Cabri* (1973), most of the analyses plot in the fields of iridosmine and osmium, rarely near the Ru–Os join (Fig. 3). Alloys corresponding to native iridium and rutheniridosmine are extremely rare; those plotting along the Ru–Ir join were not observed. The rarity of rutheniridosmine contrasts with its abundance in ophiolitic environments (especially in chromitites). However, the composition of rutheniridosmine (Table 2, analysis 2) differs from rutheniridosmines in ophiolites (*Legendre*, 1982; *Stockman* and *Hlava*, 1984; *Augé*, 1985; *Talkington* et al., 1986; *Legendre* and *Augé*, 1986; *Augé*, 1988) by significant Rh and Au concentrations.

The composition of (Os, Ru) alloys (Table 2, analyses 1 and 3) is again characterized by minor, but significant, Rh and Au concentrations. *Harris* and *Cabri* (1973) reported similar compositions for osmian ruthenium from New Guinea.

On the Os–Ir join, Os-rich phases are the most common, ranging from osmium to iridosmine (Table 2, analyses 4–9; Fig. 3). Their Ru content is generally low, exceeding only exceptionally 1 at.%. The highest Ru values seem to be restricted to the alloys richest in Ir, plotting in the osmium field (Fig. 3; Table 2). The extent of these solid solutions towards Ir is limited by the miscibility gap (*Hansen* and *Anderko*, 1958; Fig. 3). Alloys rich in Ir show the highest Cu concentrations (Table 2, analyses 7–9). The rise in the solubility of copper in Ir-rich alloys is confirmed by high copper concentrations in osmiridium and iridium, which also become Pt and Rh rich and contain exsolved Pt–Cu phases (Table 2, analyses 10–11). These phenomena are compatible with decreasing temperature of the ore-forming system.

The presence of Pt_2Cu_3 exsolution in native iridium (Table 2, analysis 11) implies that Pt and Cu concentrations in iridium, equal to 9.2 and 1.4 wt.% respectively, must be very close to the solubility limit of these elements in Ir at temperature and pressure conditions which have generated this PGE mineralization. The copper content is significantly higher than that indicated by the solubility curve of Cu in iridium at subsolidus conditions (*Berlincourt* et al., 1981). The Pt concentration (3.3 at.%) indicates a reequilibration temperature between 700° and 800° C (*Hansen* and *Anderko*, 1958), which is also inferred by the Ir content of Pt_3Fe exsolutions (see below). Taking into account this temperature range, the native iridium studied here appears to be undersaturated with respect to rhodium (*Berlincourt* et al., 1981) whose concentration drops rapidly with increasing Os content.

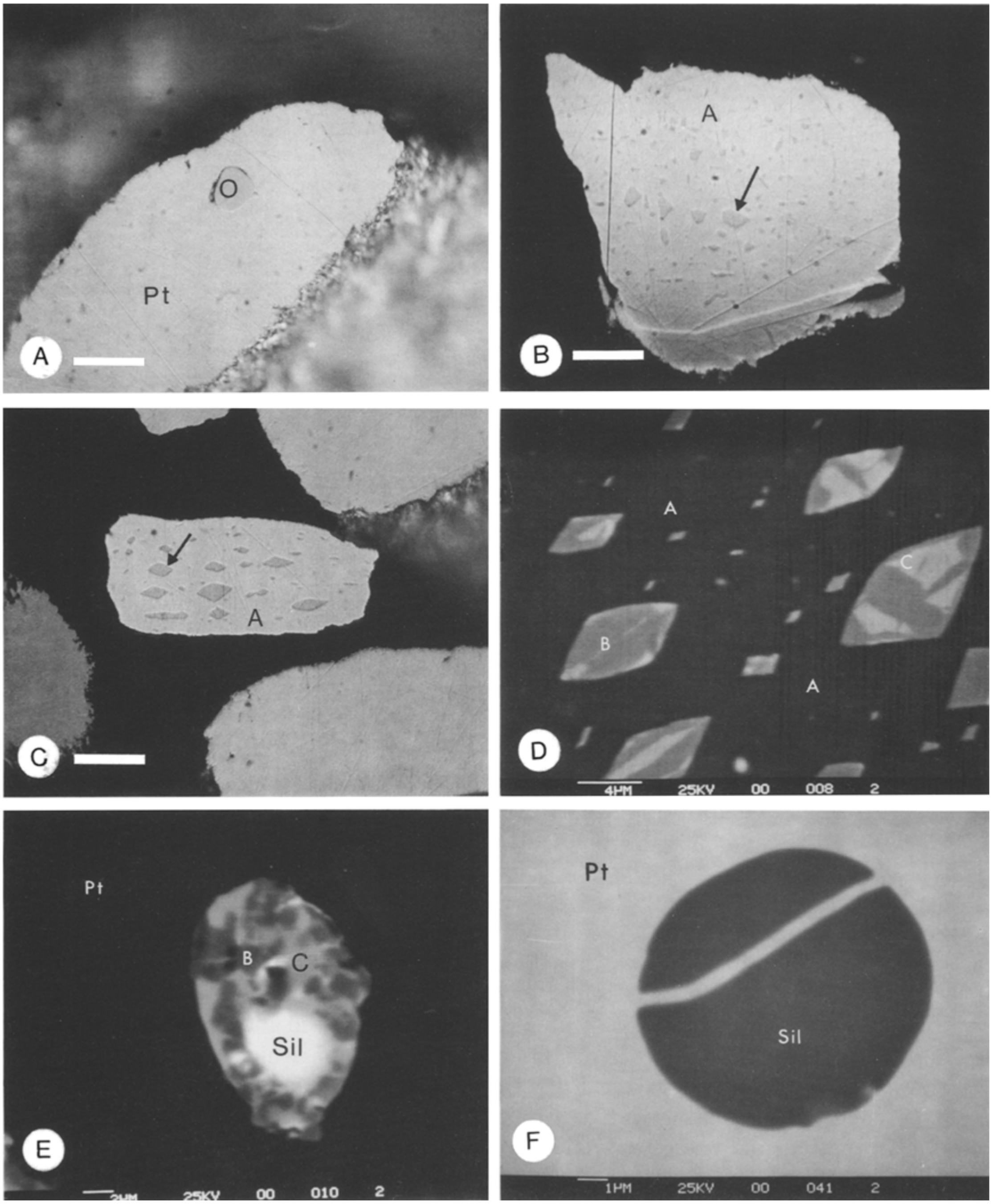

Plate 1. A) Inclusion of native osmium (*O*) in isoferroplatinum (*Pt*). B) Exsolutions of Ir-rich (Pt-Fe) alloy (arrow) in osmiridium (*A*). C) (Pt, Pd)$_2$Cu$_3$ exsolutions (arrow) in native iridium (*A*). D) (Pt, Pd)$_2$Cu$_3$ exsolutions in native iridium (*A*) observed by SEM. Two compositional fields (*B* and *C*) are observable, corresponding to the variation of Pt/Pd ratio in this intermetallic phase. E) Complex inclusion of bornite (*B*), cuprorhodsite (*C*) and silicate glass (*Sil*) in isoferroplatinum (*Pt*). F) Broken silicate-glass inclusion (*Sil*) in isoferroplatinum (*Pt*) filling fracture in the glass inclusion. A, B, C: polished section, reflected light, oil immersion; white line indicates 20 microns; D, E, F: scanning electron photomicrographs

Table 2

	1	2	3	4	5	6	7	8	9	10	11
Os	52.07	28.33	70.91	96.59	81.84	76.49	71.75	63.29	62.04	7.94	1.48
Ir	9.91	46.05	9.60	2.11	14.55	23.48	28.47	35.77	37.51	78.09	86.48
Ru	34.25	23.01	16.22	0.11	2.58	0.23	0.22	0.36	0.74	0.84	0.29
Rh	0.98	0.82	0.27	-	-	-	0.02	-	-	1.77	5.20
Pt	-	-	-	0.22	-	-	-	-	-	9.19	3.61
Pd	-	-	0.02	-	-	-	-	0.23	-	0.15	-
Fe	0.30	-	-	-	-	-	0.21	0.19	-	0.15	-
Cu	0.10	0.42	0.07	0.03	0.09	0.21	0.31	0.36	0.33	0.94	1.42
Au	0.10	0.22	0.12	-	0.22	0.15	-	0.04	0.14	0.12	0.24
Total	97.71	98.85	97.21	99.06	99.28	100.56	100.98	100.24	100.76	99.76	99.31
Os*	0.402	0.236	0.634	0.973	0.805	0.758	0.703	0.622	0.610	0.076	0.014
Ir	0.076	0.379	0.085	0.021	0.142	0.230	0.276	0.348	0.365	0.738	0.798
Ru	0.497	0.360	0.273	0.002	0.048	0.004	0.004	0.007	0.014	0.015	0.005
Rh	0.014	0.012	0.004	-	-	-	-	-	-	0.031	0.090
Pt	-	-	-	0.002	-	-	-	-	-	0.085	0.033
Pd	-	-	-	-	-	-	-	0.004	-	0.003	-
Fe	0.008	-	-	-	-	-	0.007	0.006	-	0.023	0.019
Cu	0.002	0.011	0.002	0.001	0.003	0.006	0.009	0.011	0.010	0.027	0.040
Au	0.001	0.002	0.001	-	0.002	0.001	-	-	0.001	0.001	0.002

*atomic proportions; 1,2,3,5,6,7,8,9: homogeneous grains without inclusions; 4: inclusion in isoferroplatinum (Plate 1-A); 10: matrix with exsolutions of Ir-rich isoferroplatinum (Plate 1-B); 11: matrix with exsolutions of $(Pt,Pd)_2Cu_3$ (Plate 1-C,D).

1: osmian ruthenium; 2: rutheniridosmine; 3: ruthenian osmium; 4,5: osmium; 6,7,8,9: iridosmine; 10: osmiridium (Pt-bearing); 11: iridium.

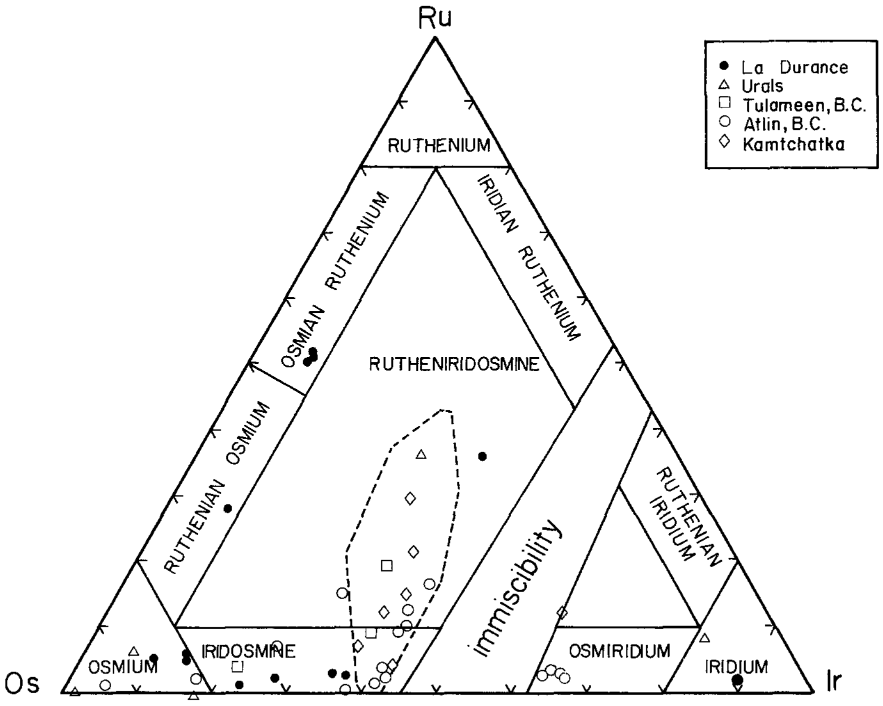

Fig. 3. Composition of (Os, Ir, Ru) alloys from the Peyrolles concentrate (●). For comparison, data from *Harris* and *Cabri*, 1973; *Zhdanov* and *Rudashevskii*, 1980 are given. The dashed line indicates the field of (Os, Ir, Ru) alloys occurring in ophiolitic chromitites (*Legendre*, 1982)

Iridium-rich Isoferroplatinum

This phase forms exsolutions in Pt-bearing osmiridium (Table 2, analysis 10). Its empirical formula (Table 4, analysis 1) may be written as $(Pt_{2.73}Ir_{0.22}Pd_{0.06}Rh_{0.04})_{3.05}(Fe_{0.91}Cu_{0.04})_{0.95}$, corresponding to Ir-bearing isoferroplatinum (*Cabri* and *Feather*, 1975). A phase of similar composition was described from the Tulameen river placers (*Cabri* and *Hey*, 1974). Disregarding minor concentrations of Os and Fe, the primordial solid solution giving rise to this exsolution should be considered as belonging to the Ir–Pt binary system. *Raub* and *Plate* (1956) have established the existence of a miscibility gap below approximately 975° C in this system.

The positioning of the miscibility curve is not known with accuracy, in particular on the Ir-rich side. However, taking into account the Ir content in the exsolved phase (7.5 at.% after correction for Fe, Cu, Pd), the solvus indicates a temperature of about 700° C. The presence of Os will probably induce a rise in the temperature of exsolution (*Hansen* and *Anderko*, 1958).

(Pt, Cu) and (Pt, Cu, Au) Alloys

Native iridium (Table 2, analysis 11) rarely contains diamond-shaped exsolutions of a Pt–Cu intermetallic phase (Table 3, analyses 3–5), crystallographically oriented with respect to the host crystal (Plate 1-C, D). The size of these exsolutions is generally less than 10 microns in their largest dimension. SEM examination in backscattered electrons reveals a two-phase field (Plate 1-D) which corresponds to Pt/Pd variation in a Pt–Cu binary compound (Table 3, analyses 3–5). One independent homogeneous grain of the same composition was observed in the studied concentrate (Table 3, analyses 1–2). A consistently low Ir concentration is attributed to interference and subtracted. The composition corresponds to an empirical formula very close to the ideal Pt_2Cu_3. Thus, a significant deficiency in platinum appears with respect to PtCu, which is the formula proposed by *Ding* (1980) for hongshiite.

Table 3

	$(Pt,Pd)_2Cu_3$				
	1	2	3	4	5
Ir	-	-	2.41	3.18	3.30
Pt	56.33	56.15	59.98	58.24	52.77
Pd	7.51	8.05	4.66	5.14	7.53
Rh	0.32	0.14	0.52	0.46	0.43
Cu	33.77	33.40	30.18	30.78	34.43
Fe	1.16	1.25	-	-	0.44
As	-	-	-	0.13	0.22
Total	99.09	98.99	97.75	97.93	99.12
Pt*	1.580	1.575	1.849	1.782	1.506
Pd	0.385	0.415	0.263	0.288	0.394
Rh	0.015	0.003	0.030	0.026	0.023
Σ	1.980	1.993	2.142	2.096	1.923
Cu	2.905	2.880	2.857	2.892	3.016
Fe	0.115	0.120	-	-	0.044
As	-	-	-	0.010	0.016
Σ	3.020	3.000	2.857	2.902	3.076

	(Pt,Pd)(Cu,Au)					
	6	7	8	9	$\bar{x}$	σ
Au	10.93	10.76	10.59	11.36	10.91	0.33
Pt	64.64	64.72	63.82	64.09	64.32	0.43
Pd	1.41	1.36	1.34	1.76	1.47	0.20
Rh	0.13	0.52	0.26	0.22	0.28	0.17
Cu	21.06	21.18	20.83	21.02	21.02	0.14
Fe	-	0.63	0.43	0.11	0.29	0.29
As	0.81	0.55	0.91	0.78	0.76	0.15
Sb	0.17	0.26	0.18	0.19	0.20	0.04
Total	99.15	99.98	98.36	99.53	99.25	
Au**	0.148	0.144	0.144	0.154	0.148	
Pt	0.890	0.874	0.878	0.876	0.880	
Pd	0.036	0.034	0.034	0.044	0.036	
Rh	0.004	0.014	0.006	0.006	0.008	
Cu	0.890	0.880	0.880	0.882	0.882	
Fe	-	0.030	0.020	0.006	0.014	
As	0.028	0.020	0.032	0.028	0.026	
Sb	0.004	0.006	0.004	0.004	0.004	

1,2: independent grain; 3,4,5: exsolution in native iridium

*number of atoms calculated for 5 atoms per formula unit after subtraction of Ir for the analyses 3 to 5

** number of atoms calculated for the total of 2 atoms per formula unit

Although this compound has not been reported from the Pt–Cu binary system (*Hansen* and *Anderko*, 1958), the investigation of order-disorder changes has shown that these transformations take place in a very large compositional range (35–55 at.% Pt) around PtCu, the highest degree of ordering being attained at 50 at.% Pt (*Schneider* and *Esch*, 1944). The average $\Sigma(\mathrm{Pt, Pd, Rh}) \approx 40$ at.% falls in the range of compositions where the cubic unit-cell is deformed in a rhombohedral structure. The shape of exsolutions (Plate 1-C, D) agrees well with trigonal symmetry. Although it was not possible to perform an X-ray study of this phase, the microprobe analyses and the Pt–Cu phase diagram (*Hansen* and *Anderko*, 1958) indicate the plausibility of a variation of Pt/Cu ratio around the ideal PtCu composition for natural alloys. According to *Assayag* and *Dodé* (1954), the ordering temperature of the (Pt, Cu) alloy with ≈ 40 at.% Pt is about 800° C, but this composition falls in a two-phase field due to the fact that the ordering of PtCu is a first-order reaction.

One free grain of ternary (Pt, Cu, Au) alloy was observed. The average of microprobe analyses (Table 3, analyses 6–9) corresponds to the empirical formula $(\mathrm{Pt_{0.88}Pd_{0.04}Fe_{0.01}As_{0.03}Rh_{0.01}})_{0.97}(\mathrm{Cu_{0.88}Au_{0.15}})_{1.03}$, suggesting an ordered alloy with distorted CuAu-type structure (*Hansen* and *Anderko*, 1958). Natural Pt–Cu–Au alloys are extremely rare. *Aubut* (1979) reported a (Pt, Cu, Au) alloy included in tulameenite from the Tulameen river PGM-concentrate.

Cuprorhodsite

Cuprorhodsite, included in (Pt, Fe) alloys, is generally associated with bornite (Plate 1-E; Plate 2-A, B, C, D), rarely with Pd-rich phases. It forms euhedral to subhedral crystals (maximum 20 microns) preferentially oriented with respect to the host-(Pt, Fe) alloy (Plate 2-C). This suggests that cuprorhodsite originated by exsolution from a complex Pt–Rh–Cu–Fe solid solution enriched in sulphur. The presence of an intimate intergrowth with bornite (Plate 1-E; Plate 2-A) indicates the possibility of a multi-stage exsolution process. Selected microprobe analyses are given in Table 4. They confirm the chemical formula $\mathrm{Cu(Rh, Ir, Pt)_2S_4}$, proposed by *Rudashevskii* et al. (1985) and show large compositional variation. Two compositional trends may be distinguished:

a. Solid solution along the $\mathrm{CuRh_2S_4}$–$\mathrm{CuPt_2S_4}$ join, with $\mathrm{CuIr_2S_4}$ lower than 1 mol.% (Fig. 4). The malanite (*Yu* et al., 1974) mole fraction varies from 11.7 to 24.7 mol.%. Some analyses show significant Pd concentrations (up to 2.8 wt.%). Tetrahedral sites are essentially occupied by Cu and Fe, but Ni is consistently present (about 4% of the site occupancy as a maximum). The iron content approaches 40% of the site occupancy. Cuprorhodsite from the Far East of the USSR exhibits similar iron concentrations (*Rudashevskii* et al., 1985).

b. Solid solution characterized by a high molar fraction of cuproiridsite, negatively correlated with the $\mathrm{CuRh_2S_4}$ end-member (Fig. 4). Implicitly, the concentration of the malanite end-member is almost constant. The occupancy of tetrahedral sites by Cu is much higher, up to 82%; nickel concentrations are systematically very low.

PGE- and Cu-Bearing Arsenides

Droplet-like inclusions composed of intimate intergrowths of arsenides occur rarely within isoferroplatinum (Plate 2-E). Their size is generally less than 4 microns,

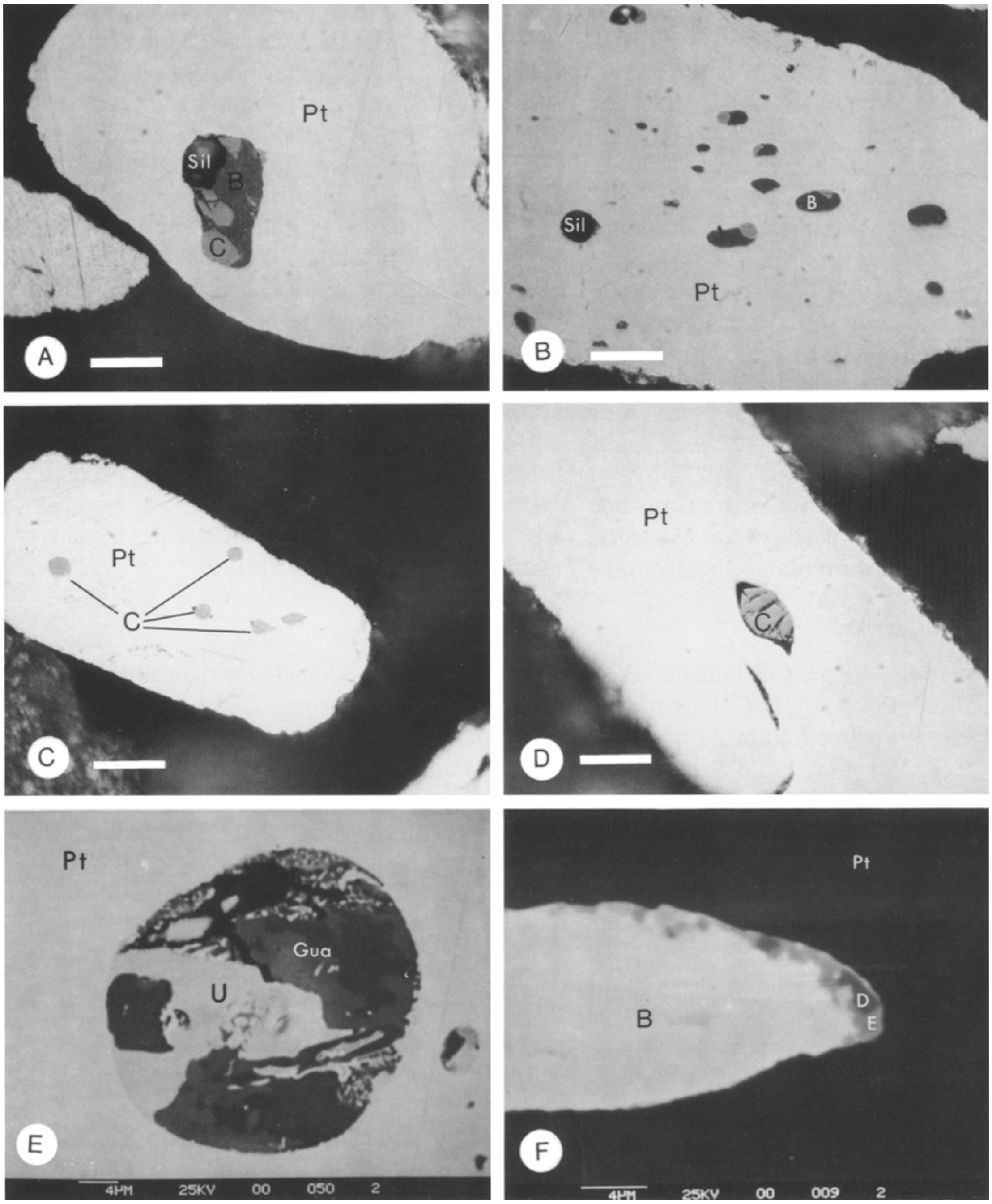

Plate 2. A) Bornite (*B*) and silicate-glass inclusion (*Sil*) in isoferroplatinum (*Pt*). Bornite contains euhedral crystals of cuprorhodsite (*C*). B) Droplet-like inclusions of bornite (*B*) with cuprorhodsite (grey) in isoferroplatinum (*Pt*). *Sil* silicate glass inclusion. C) Cuprorhodsite (*C*) associated with traces of bornite (dark grey) in isoferroplatinum (*Pt*). D) Cuprorhodsite crystal (*C*) inclusion in isoferroplatinum (*Pt*). Pressure shadow around cuprorhodsite indicates strong deformation of isoferroplatinum. E) Complex, droplet-like, inclusion of guanglinite (*Gua*) with variable Pt/Pd ratio and of an unknown phase $(Pt, Pd)_{4+x}Cu_2As_{1-x}$(*U*) in isoferroplatinum (*Pt*). F) Bornite inclusion (*B*) rimmed by Pd telluride (*D*) and Pd-Cu sulphide (*E*), in isoferroplatinum (*Pt*). A, B, C, D: polished section, reflected light, oil immersion; white line indicates 20 microns; E, F: scanning electron photomicrographs

Table 4

	1	2	3	4
Ir	6.51	-	-	-
Ru	0.03	-	-	0.04
Rh	0.59	11.62	0.27	-
Pt	81.77	13.40	0.16	0.61
Pd	0.95	42.40	-	-
Fe	7.82	2.24	10.88	6.65
Ni	-	0.05	0.05	-
Cu	0.45	10.19	60.76	64.76
Au	-	0.18	0.07	-
S	0.04	16.34	25.31	24.20
Total	98.06	96.42	97.50	96.26
Ir*	0.055	-	-	-
Ru	0.001	-	-	0.002
Rh	0.009	0.087	0.013	-
Pt	0.680	0.053	0.004	0.016
Pd	0.014	0.308	-	-
Fe	0.227	0.031	0.987	0.631
Ni	-	0.001	-	-
Cu	0.011	0.124	4.846	5.402
Au	-	0.001	-	-
S	0.002	0.394	4	4

	5	6	7
Ir	0.55	0.74	23.48
Ru	-	0.46	0.14
Rh	42.15	33.33	19.93
Pt	10.71	18.38	14.86
Pd	-	1.40	0.40
Cu	9.29	9.49	9.91
Fe	5.63	4.70	3.01
Ni	0.35	0.52	0.07
S	31.27	28.78	26.77
Total	99.95	97.80	98.57
Ir*	0.012	0.017	0.585
Ru	-	0.020	0.006
Rh	1.680	1.444	0.928
Pt	0.224	0.420	0.365
Pd	-	0.059	0.018
Cu	0.600	0.666	0.747
Fe	0.412	0.375	0.259
Ni	0.024	0.040	0.006
S	4	4	4

*number of atoms calculated on the basis of 1 atom per formula unit (analyses 1,2) and of 4 S (analyses 3-7); 1: exsolution in osmiridium (Table 2, analysis 10); 2: Pd-, Cu-sulphide associated with cuprorhodsite and included in isoferroplatinum; 3: bornite associated with cuprorhodsite and included in isoferroplatinum; 4: bornite associated with Pd-, Cu-sulphide and Pd telluride, and included in isoferroplatinum; 5-7: cuprorhodsite included in isoferroplatinum.

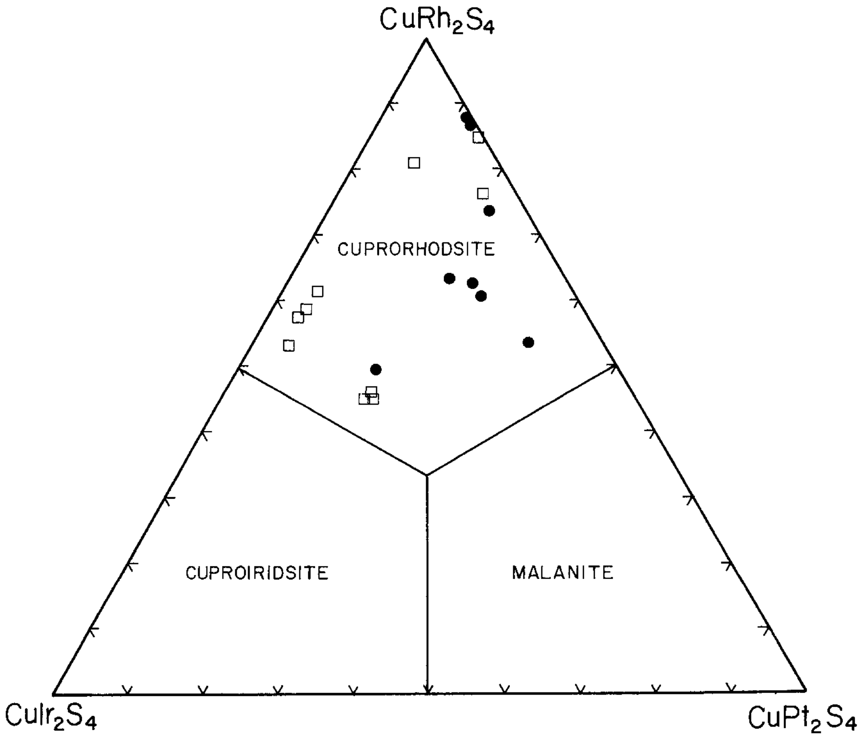

Fig. 4. Plot of chemical compositions of cuprorhodsite from the Peyrolles concentrate (●). ☐ Cuprorhodsite from the Far East of the USSR (*Rudashevskii* et al., 1985)

Table 5

	$(Pt,Pd)_{4+x}Cu_2As_{1-x}$					$(Pd,Pt)_3(As,Sb)$		
	1	2	3	$\bar{x}$	σ	4	5	6
Pt	74.28	73.50	74:17	73.98	0.42	25.40	26.68	41.95
Pd	5.15	5.36	5.07	5.19	0.15	53.59	51.56	39.79
Rh	0.27	0.17	0.06	0.17	0.10	0.00	0.00	0.33
Cu	12.40	12.29	12.54	12.41	0.12	0.28	0.44	2.00
Fe	0.41	0.29	0.13	0.28	0.14	0.00	0.00	0.00
As	5.71	5.73	5.64	5.69	0.05	14.15	14.24	13.35
Sb	0.13	0.09	0.02	0.08	0.05	2.56	2.60	1.73
Total	98.35	97.43	97.63	97.80		95.98	95.52	99.15
Pt	3.746*	3.743	3.782	3.757		0.614**	0.652	1.054
Pd	0.476	0.500	0.474	0.483		2.375	2.308	1.833
Rh	0.026	0.017	0.006	0.016		-	-	0.016
Cu	1.919	1.921	1.964	1.935		0.021	0.033	0.154
Fe	0.073	0.051	0.023	0.049		-	-	-
As	0.750	0.760	0.749	0.753		0.890	0.906	0.874
Sb	0.010	0.008	0.002	0.007		0.099	0.102	0.070

* calculated for 7 atoms per formula unit

** calculated on the basis of 4 atoms per formula unit

exceptionally reaching up to 30 microns. Two different phases were distinguished in reflected light in oil immersion:

A. a grey phase having a reflectance slightly lower than isoferroplatinum;

B. a cream-coloured phase, much softer than phase A and isoferroplatinum, with a moderately high reflectance. The small size of these minerals prevented the determination of other optical properties in reflected light.

SEM study (Plate 2-E) revealed that phase A contains Pt, Pd, Cu As and phase B contains Pt, Pd, As, Sb, as major elements. Furthermore, phase B is compositionally heterogeneous, exhibiting a strong variation in Pt/Pd ratio. Microprobe analyses (Table 5) gave generally low totals, which may be explained by extreme operating conditions due to the small grainsize of the minerals analysed. The chemical composition of phase A (Table 5, analyses 1–3) is characterized by an average $(Me/As)_{at}$ ratio equal to 8.21. However, when calculated on the basis of 7 atoms per formula unit, $\Sigma(Cu, Fe)$ is close to 2 and the average formula can be written $(Pt_{3.76}Pd_{0.48}Rh_{0.02})_{4.26}(Cu_{1.93}Fe_{0.05})_{1.98}(As_{0.75}Sb_{0.01})_{0.76}$, or more generally $(Pt, Pd)_{4+x}Cu_2As_{1-x}$, with $x \approx 0.25$. This suggests a formula unit containing 28 atoms and giving $(Pt_{15.03}Pd_{1.93}Rh_{0.06})_{17.02}(Cu_{7.74}Fe_{0.20})_{7.94}(As_{3.01}Sb_{0.03})_{3.04}$ or ideally $(Pt, Pd)_{17}Cu_8As_3$. None of the known PGE minerals correspond to this composition.

Phase B (Table 5, analyses 4–6) is much richer in Pd and As compared with phase A; a significant Sb concentration is noteworthy. The chemical composition is close to $(Pd, Pt)_3(As, Sb)$, with $Pd/(Pd + Pt)_{at}$ ranging from 0.79 to 0.63. Cu concentration remains low and Fe is systematically below the microprobe detection limit. These results, as well as the incomplete optical data, are compatible with published data for guanglinite (*Yu* et al., 1974), identical with the synthetic phase Pd_3As (*Shunk*, 1969). However, an extensive solid solution with a hypothetical platinum end-member, Pt_3As, is observed, but this phase is unknown in the Pt-As binary system.

Palladium-rich Phases

The composition of (Pt, Fe) alloys (Table 1) and of cuprorhodsite (Table 4) indicates a significant activity of Pd in the ore-forming system. However, palladium minerals are very rare in the concentrate studied.

SEM study of bornite inclusions revealed the presence of a palladium telluride associated with a Pd-Cu sulphide and forming a thin rim around the bornite inclusion (Plate 2-F). Although microprobe analysis was not possible, this observation indicates the presence of tellurium in the ore-forming system. An enrichment of the bornite solid solution in Te at higher temperature is suggested.

Cuprorhodsite was also found associated with a Pd-rich sulphide. In reflected light, in oil, the mineral has a grey colour with a brownish shade compared with cuprorhodsite. Its reflectivity is only slightly higher than that of cuprorhodsite; this difference becomes observable in oil immersion only. Neither internal reflections nor anisotropy were observed. Microprobe analysis (Table 4, analysis 2) reveals a complex composition with an Me/S atomic ratio equal to 1.53. The empirical formula calculated on the basis of 5 atoms is $(Pd_{1.54}Cu_{0.62}Rh_{0.44}Pt_{0.27}Fe_{0.15})_{3.02}S_{1.98}$, which may be rearranged as $(Cu_{0.62}Fe_{0.15})_{0.77}(Pd_{1.54}Rh_{0.44}Pt_{0.27})_{2.25}S_{1.98}$. Consequently, the ideal formula of this mineral can be written as $(Cu,Fe)_{1-x}(Pd,Rh,Pt)_{2+x}S_2$. No phase of this composition is known in the Pd–Cu–S system (*Berlincourt* et al., 1981). It is interesting to note that an unnamed mineral with formula $CuPd_4S_2$ was observed in placers related to ultramafics from the Far East of the USSR (*Rudashevskii* et al., 1985).

Native Gold and (Au, Ag, Cu) Alloys

Native gold and gold alloys with Ag, Cu, Pd and Pt were found in several PGM deposits and placers (*Borisenko* et al., 1969; *Cabri* and *Laflamme*, 1974; *Razin*, 1975; *Schwellnus* et al., 1976; *Toma* and *Murphy*, 1978; *Aubut*, 1979; *Ramdohr*, 1980; *Zhdanov* and *Rudashevskii*, 1980; *Novgorodova*, 1983; *Krendelev* et al., 1986). In the Durance river PGM concentrate, these phases appear as free grains devoid of silicate inclusions. In one case only, the association of (Au, Ag, Cu) alloy with Ni, Cu sulphides (heazlewoodite and an undetermined phase) was observed. Furthermore, the presence of Ni-, Sn-, Pb-, Pt- and Pd-bearing inclusions in (Au, Cu, Ag) alloys, as well as the gold concentration found in (Os, Ir, Ru) alloys (Table 2) and in a Pd-rich sulphide (Table 4), indicate a unique source for gold-bearing phases and for PGM in this concentrate.

Selected microprobe analyses of Au and (Au, Cu, Ag) alloys are given in Table 1. Two different compositional groups may be distinguished:

a. Native gold with Ag-content less than 1 at.% (analysis 1) and (Au, Ag) alloys containing up to (at.%) 13.6 Ag and 10.0 Cu. Pt and Pb are present in most cases. Rarely, significant tin values have been detected, accompanied by Pb, Ni and Fe in a grain exhibiting minute inclusions of shandite and Pt-, Ni-, Sn-bearing phases (Table 1).

b. (Au, Ag, Cu) alloys. They show variable concentrations of Ag and Cu, but their Au content is rather constant, close to 50 at.%. Empirical formulae are close to the ideal composition Au(Cu, Ag), which corresponds to silver-bearing tetrauricupride, the natural equivalent of ordered AuCu (*Novgorodova*, 1983). Minor concentrations of Ni and Fe are invariably present; Pb and Sn appear in some cases, and the concentration of Sn can reach several wt.% (Table 1). Neither Pt nor Pd were detected. It is interesting to note that in the Au–Cu system alloys with 50 to 60 at.% Au lie near the liquidus minimum at about 900° C. The ordering of AuCu takes place at temperatures as low as 400° C (*Hansen* and *Anderko*, 1958).

Shandite

Several minute inclusions of a Pb- and Ni-bearing sulphide were observed in an (Au, Ag, Cu) alloy. The largest (3 × 2 microns) was analysed by microprobe (Table 6). After subtracting the matrix, the composition corresponds to $(Ni_{2.86}Sn_{0.15}Cu_{0.03}Pd_{0.01})_{3.05}Pb_{2.06}S_2$, very close to the ideal formula of shandite.

This very rare mineral was discovered, associated with heazlewoodite, sphalerite and chromite, in a serpentinized ultramafic at Trial Harbor, Tasmania (*Ramdohr*, 1949). Since then, its occurrence was described only twice (*Nickel* et al., 1979; *Dymek*, 1987). *Genkin* et al. (1983) described a rhodium equivalent of shandite, named rhodplumbite, associated with Cu-bearing platinum in placers from the Urals. Consequently, its presence in the Durance river concentrate points towards an ultramafic source of the (Au, Ag, Cu) alloys.

Table 6

	shandite				(Ni,Pt)Sn			
	1	2	3	4	1	2	3	4
Ni	18.55	0.09	24.68	2.859	7.19	0.24	29.30	0.942
Pb	47.06	0.06	62.84	2.062	0.48	0.16	1.35	0.012
Cu	1.21	0.99	0.29	0.031	2.80	2.76	0.17	0.005
Sn	2.15	0.20	2.61	0.149	14.00	0.54	56.75	0.902
Ag	0.55	0.55	-	-	4.23	4.23	-	-
Pd	0.09	-	0.12	0.008	0.53	-	2.23	0.039
Pt	0.02	-	0.03	0.001	2.42	-	10.20	0.099
Au	23.78	23.78	-	-	66.34	66.34	-	-
S	7.05	-	9.43	2	-	-	-	-
Σ	100.46		100		97.99		100	

1-microprobe analysis; 2-subtraction of matrix (analysis 5, Table 5); 3-composition recalculated to 100%; 4-number of atoms per formula unit calculated on the basis of 2 S (shandite) and for the total of 2 atoms (compound (Ni,Pt)Sn)

(Ni, Pt)Sn

A detailed investigation of the (Au, Cu, Ag) alloy containing shandite showed the presence of Pt-rich submicroscopic inclusions (≈ 2 microns in diameter), also enriched in Ni and Sn. Microprobe analysis led to the empirical formula $(Ni_{0.94}Pt_{0.10} \cdot Pd_{0.04})_{1.08}(Sn_{0.90}Pb_{0.01})_{0.91}$, approaching (Ni, Pt)Sn. The compound NiSn is unknown in the Ni–Sn system. However, the phase reported as Ni_3Sn_2 has a hexagonal NiAs-type structure, being isostructural with PtSn and PtPb (*Hansen* and *Anderko*, 1958). This could indicate the possibility of extensive solid solutions between these compounds and explain the presence of Pt and Pb, revealed by microprobe analyses.

The chemical composition of the (Au, Ag, Cu) host-alloy is characterized by minor concentrations of Ni, Fe, Sn and Pb. This shows that shandite and (Ni, Pt)Sn inclusions might result from an exsolution process induced by the miscibility gap between Au and Ni at lower temperatures (*Münster* and *Sagel*, 1958). This hypothesis is corroborated by the absence of Sn-rich exsolutions in Sn-bearing (Au, Ag, Cu) alloys devoid of nickel (Table 1, analysis 5). The nickel concentration (0.96 wt.%) in the (Au, Ag, Cu) alloy coexisting with nickel sulphide, indicates a rather low temperature of reequilibration (≈ 400° C) according to *Münster* and *Sagel* (1958).

Minerals belonging to Pt-Sn and Pd-Sn systems were reported from all the major PGE deposits (Merensky Reef, Stillwater, Norilsk, Sudbury; *Cabri*, 1981). At

Norilsk, Sn- and Pb-bearing PGM are late and commonly associated with native gold (*Genkin*, 1968). Similar paragenetic relationships in the ore-system which led to the Durance river PGM association might explain the absence of Pt_3Fe inclusions in native gold and in (Au, Ag, Cu) alloys.

Bornite

Bornite is the only base-metal sulphide occurring as inclusion in (Pt, Fe) alloys in the studied concentrate. It is generally associated with PGE sulphides and tellurides (Plate 1-E; Plate 2-A, B, F). In places, bornite inclusions containing PGE-bearing phases are intimately associated with silicate-glass inclusions (Plate 1-E).

Microprobe analyses are of poor quality, due to the very small size of the inclusions (Table 4); they reveal either a composition close to stoichiometry (analysis 3), or show an important excess of Cu (analysis 4). The presence of Rh and Pt is probably due to cuprorhodsite and an isoferroplatinum-host respectively. The presence of bornite with excess copper indicates an extensive solid solution towards digenite, formed at higher temperature and stabilized by rapid cooling (*Cabri*, 1973). This "anomalous" bornite is usually associated with Pd sulphides and tellurides (see above), in agreement with a higher solubility of these elements in bornite solid solution at high temperature.

Silicate-Glass Inclusions

Besides various PGM, silicate-glass droplets were observed as inclusions in (Pt, Fe) alloys. They are generally about 10 microns in size. SEM and Raman probe investigations revealed that some of them are partly devitrified. The detailed study of silicate-glass inclusions in (Pt, Fe) alloys will be published elsewhere (*Ohnenstetter* and *Johan*, in prep.).

Microprobe analyses showed SiO_2 ranging from 44 to 63 wt.%. Different petrological plots indicate the composition varying from basaltic to dacitic, with a majority of compositions falling in the andesitic field. We believe that the low TiO_2 content is characteristic of orogenic-type magmatic suites. Some inclusions are K-rich, plotting in the shoshonitic field. Minor Cl, F and P_2O_5 concentrations were detected by microprobe.

As is obvious from Plate 1-F, certain inclusions were already solid when the (Pt, Fe) alloys formed. This is an important indication of the maximum temperature limit for the deposition of (Pt, Fe) alloys, which is definitely lower than the solidus temperature of these glass inclusions.

Discussion

The PGM concentrate from Peyrolles shows the following mineralogical and chemical characteristics:

a. —predominance of (Pt, Fe) alloys (92%) over (Os, Ir, Ru) alloys (3.5%);
b. —within the latter, the abundance of binary Os–Ir and Ru–Os alloys contrasts with the rarity of ternary alloys (rutheniridosmine);
c. —absence of mineral inclusions in (Os, Ir, Ru) alloys;
d. —abundance of metallic minerals and silicate-glass inclusions in isoferroplatinum and their absence in the ferroan platinum;

e. —(Pt, Fe) alloys systematically exhibit relatively high Rh, Pd and Cu concentrations; the iridium content can reach up to 2 wt.%, but exsolutions of Ir-rich phases have not been observed; furthermore, (Pt, Fe) alloys are strongly depleted in Os;
f. —although the true proportion of native gold in the concentrate could not be estimated due to the amalgamation of the heavy-mineral concentrate, the abundance of (Au, Cu) alloys is noteworthy. The presence of Pt-bearing inclusions in the latter, as well as the occurrence of (Pt, Cu, Au) alloys indicate a single source for PGM's and gold-bearing alloys.

The observations presented point towards a well-defined ore-forming system; relevant aspects are summarized below.

1. The low Ru contents, and particularly the absence of laurite and the paucity of rutheniridosmine, are incompatible with a PGM source related to ophiolitic chromitites (*Legendre*, 1982; *Legendre* and *Augé*, 1986; *Talkington* et al., 1986; *Tarkian* and *Prichard*, 1987; *Thalhammer* and *Stumpfl*, 1988).

2. The inclusions of native osmium in (Pt, Fe) alloys (Plate 1-A), clearly indicate the early crystallization of Os, Ir and Ru-rich phases. This can explain the depletion in these elements observed in (Pt, Fe) alloys. However, the absence of laurite indicates either a high temperature, which is incompatible with the entire association, or prior partial extraction of Ru in form of laurite by another Pt-bearing ore-forming system, which did not contribute to the Durance river basin. This system should also have been enriched in Ir, according to the extensive Pt–Ir miscibility at high temperature (*Hansen* and *Anderko*, 1958).

3. The composition of (Pt, Fe) alloys and included mineral phases indicates a PGE source considerably enriched in Rh and Cu. This kind of enrichment is atypical of PGE-mineralization related to ophiolites and stratiform intrusions, but is highly characteristic of Alaskan-type intrusive complexes (*Cabri* et al., 1973; *Zhdanov* and *Rudashevskii*, 1980; *Rudashevskii* and *Zhdanov*, 1983; *Rudashevskii*, 1984; *Johan* et al., 1989). The presence of (Pt, Cu) alloys and bornite inclusions in (Pt, Fe) alloys was reported from several Alaskan-type PGE mineralizations (*Yu* et al., 1974; *Aubut*, 1979; *Ding*, 1980; *Ramdohr*, 1980; *Cabri* et al., 1981). This statement is corroborated by the strong predominance of iridosmine in the Peyrolles concentrate.

4. The presence of cuprorhodsite and bornite exsolutions in (Pt, Fe) alloys, associated with minor Pd-bearing phases, suggests a complex solid solution of Pt, Fe, Ir, Rh, Pd, Cu, Ni, Au and S at high temperatures. The droplet-like shape of bornite exsolutions in isoferroplatinum (Plate 2-A, B) indicates a sulphur-rich, Cu-, Fe-, and PGE-enriched liquid; experimental aspects of this liquid have been demonstrated by *Makovicky* et al. (1986), who showed that it undergoes a subsolidus evolution leading, at about 600° C, to the appearance of cuprorhodsite. The presence of tellurium in this liquid gave rise to palladium tellurides (Plate 2-F), formed at relatively low temperatures from the intermediate Cu–Fe–S solid solution (iss).

As-rich and S-free, Pt, Pd and Cu-bearing liquid occurs rarely in isoferroplatinum (Plate 2-E). Its subsolidus evolution leads to a complex association of arsenides. The predominant phase, $(Pd, Pt)_3As$, melts at about 830° C (*Shunk*, 1969); consequently, this temperature must be considered as the minimum entrapment temperature for this liquid. The presence of two types of liquids indicates the concentration of highly volatile elements, and the existence of complex solid-liquid and probably also liquid-liquid immiscibility phenomena in the ore-forming system.

5. The high activity of Cu is also revealed by (Pt, Cu) alloys (Plate 1-C, D), and by the presence of (Pt, Cu, Au) and (Au, Cu) alloys. Among the various types of PGE mineralization, those related to Alaskan-type intrusions show the highest Cu concentrations in (Pt, Fe) alloys which are sometimes associated with Pt–Cu and Pt–Cu–Fe intermetallic phases (*Razin* and *Yurkina*, 1971; *Cabri* et al., 1973; *Fominykh* et al., 1974; *Begizov* et al., 1975; *Voltchenko* et al., 1975; *Ding*, 1980). *Rudashevskii's* (1984) statistical study on the chemistry of (Pt, Fe), and (Os, Ir, Ru) alloys showed that (Pt, Fe) alloys occurring in "dunite-clinopyroxenite" and "alkaline-type" complexes are considerably enriched in Cu.

Zhdanov and *Rudashevskii* (1980) and *Rudashevskii* and *Zhdanov* (1983) described a PGE mineralization related to mafic-ultramafic Alaskan-type intrusions of Devonian age from the northern border of the Kamchatka Precambrian Shield. The PGM association is characterized by the predominance of Ir-poor and Rh-enriched isoferroplatinum. Among (Os, Ir, Ru) alloys, the preponderance of osmiridium and iridosmine should be noted. Isoferroplatinum bears inclusions of Rh-rich phases (cuprorhodsite—cuproiridsite solid solution) and palladium sulphides. PGM's are associated with (Au, Cu) alloys and native gold. Silicate inclusions are commonly K-rich phases. This paragenesis strikingly resembles the PGM association found in the Durance river alluvium.

6. The almost constant thickness of most of the flattened (Pt, Fe) alloy particles in the concentrate studied suggests their deformation during a metamorphic event. This is corroborated by the appearance of a "pressure shadow" around rigid cuprorhodsite inclusions, which also exhibit open fractures perpendicular to the flattening (Plate 2-D). Assuming the primarily cubic habit of (Pt, Fe) alloy crystals (Fig. 1A) with (100) edges close to 130 microns in length, and taking into account the average dimension of (Pt, Fe) discoidal particles, the flattening factor (width/thickness) approaches 2.

In conclusion, it seems highly probable that the primary source of the PGM association in the Durance river alluvium is an Alaskan-type intrusion, metamorphosed under highly dynamic conditions. The intrusion later might have been tectonically dismembered and completely eroded. Considering the strong wear observed on some of these hard alloys, derivation of the PGM association from a paleo-placer cannot be excluded at this stage of the research.

Acknowledgements

We would like to thank *C. Urtin* who discovered the PGM in the Durance river alluvium and who kindly provided the concentrate for this study. Thanks are due to *C. Gilles* (BRGM) and *D. Ohnenstetter* (CNRS) for careful analytical work. We wish also to acknowledge the PIRSEM (CNRS) for financial support through the ATP "Gîtologie" to *M. Ohnenstetter* and *J. Amossé*, *H. M. Kluyver* (BRGM) who improved the English of the manuscript, and two anonymous reviewers for constructive comments. This work is part of a research project of the BRGM on "Mineralizations related to mafic and ultramafic rocks".

References

Assayag P, Dodé M (1954) Etude thermodynamique expérimentale de la surstructure platine, cuivre PtCu. CR Acad Sci Paris 239: 762–764

Aubut AJ (1979) The geology and mineralogy of a Tertiary buried placer deposit, southern British Columbia. M Sc Thesis Univ of Alberta

Augé T (1985) Chromitites et minéraux du groupe du platine dans les complexes ophiolitiques. Unpubl Thesis Univ Orléans, 270 p

— (1988) Platinum-group minerals in the Tiébaghi and Vourinos ophiolitic complexes: genetic implications. Canad Mineral 26: 177–192

Begizov VD, Borisenko LF, Uskov ED (1975) Sulphides and natural solid solutions of platinoids from the Gusevogorsk ultramafic complex (the Urals). Dokl Akad Nauk SSSR 225: 1408–1411 (in Russian)

Berlincourt LE, Hummel HH, Skinner BJ (1981) Phases and phase relations of the platinum-group elements. In: *Cabri LJ* (ed) Platinum-group elements: mineralogy, geology, recovery. CIM spec vol 23: 19–45

Borisenko LF, Uskov ED, Lutchin NS (1969) Accessory minerals and minor elements in hornblendites of the Gusevogorsk massif. Izv Akad Nauk SSSR, Ser geol No 1: 83–96 (in Russian)

Cabri LJ (1973) New data on phase relations in the Cu–Fe–S system. Econ Geol 68: 443–454

— (1981) The platinum-group minerals. In: *Cabri LJ* (ed) Platinum-group elements: mineralogy, geology, recovery. CIM spec vol 23: 85–150

— *Criddle AJ, Laflamme JHG, Bearne GS, Harris DC* (1981) Mineralogical study of complex Pt–Fe nuggets from Ethiopia. Bull Minéral 104: 508–525

— *Feather CE* (1975) Platinum-iron alloys: a nomenclature based on a study of natural and synthetic alloys. Canad Mineral 13: 117–126

— *Harris DC* (1975) Zoning in Os–Ir alloys and the relation of the geological and tectonic environment of the source rocks to the bulk Pt/(Pt + Ir + Os) ratio for placers. Canad Mineral 13: 266–274

— *Hey MH* (1974) Platiniridium—confirmation as a valid mineral species. Canad Mineral 12: 299–303

— *Laflamme JHG* (1974) Rhodium, platinum and gold alloys from the Stillwater complex. Canad Mineral 12: 339–403

— *Owens DR, Laflamme JHG* (1973) Tulameenite, a new platinum-iron-copper mineral from placers in the Tulameen river area, British Columbia. Canad Mineral 12: 21–25

Ding K (1980) Further studies of the minerals “isoplatincopper” and “hongshiite” Scient Geol Sin No 2: 168–171 (in Chinese)

Dymek RF (1987) Shandite, $Ni_3Pb_2S_2$, in a serpentinized metadunite from the Isua supracrustal belt, West Greenland. Canad Mineral 25: 245–249

Fischer W, Amossé J, Begon P, Urtin C (1988) Découverte d'isoferroplatine, Pt_3Fe, dans les alluvions aurifères de la Durance, Sud-Est de la France. CR Acad Sci Paris 307: 1061–1066

Fominykh VG, Yushko-Zakharova OE, Dubakina LS (1974) Platinum-group minerals of the Gusevogorsk deposit. Dokl Akad Nauk SSSR 217: 663–666 (in Russian)

Genkin AD (1968) Minerals of platinum-group metals and their associations in copper-nickel ores of the Norilsk deposit. Nauka Moscow, 105 p (in Russian)

— *Vjalsov LN, Evstigneeva TL, Laputina IP, Basova GV* (1983) Rhodplumbite $Rh_3Pb_2S_2$, a new sulphide of rhodium and lead. Mineral Zhurn 1983, No 2: 87–91 (in Russian)

Gueymard E (1853) Recherches analytiques du platine dans les Alpes. Procès-verbal des délibérations du Conseil général du Département de l'Isère: 483–515

Hansen M, Anderko K (1958) Constitution of binary alloys. McGraw-Hill Book Company Inc, New York Toronto London, 1305 p

Harris DC (1974) Ruthenarsenide and iridarsenide, two new minerals from the Territory of Papua and New Guinea and associated irarsite, laurite and cubic iron-bearing platinum. Canad Mineral 12: 280–284

— *Cabri LJ* (1973) The nomenclature of the natural alloys of osmium, iridium and ruthenium based on new compositional data of alloys from world-wide occurrences. Canad Mineral 12: 104–112

Johan Z, Ohnenstetter M, Slansky E, Barron LM, Suppel D (1989) Platinum mineralization in the Alaskan-type intrusive complexes near Fifield, New South Wales, Australia. Part 1. Platinum-group minerals in clino-pyroxenites of the Kelvin Grove prospect, Owendale intrusion. Mineral Petrol 40: 289–309

Krendelev FP, Genkin AD, Laputina IP, Rugovik GI (1986) Pt-bearing gold in placers related to granulitic rocks of an Archean complex. Dokl Akad Nauk SSSR 291: 960–963 (in Russian)

Legendre O (1982) Minéralogie et géochimie des platinoïdes dans les chromitites ophiolitiques. Unpubl Thesis Univ Paris VI, 171 p

— *Augé T* (1986) Mineralogy of platinum-group mineral inclusions in chromitites from different ophiolitic complexes. In *Gallagher* et al. (eds) Metallogeny of basic and ultrabasic rocks, IMM, London, 361–372

Makovicky M, Makovicky E, Rose-Hansen J (1986) Experimental studies on the solubility and distribution of platinum-group elements in base-metal sulphides in platinum deposits. In: *Gallagher* et al. (eds) Metallogeny of basic and ultrabasic rocks. IMM, London, 415–425

Münster A, Sagel K (1958) Separation curve and critical point of the system gold–nickel. Zeit physik Chem (Frankfurt) 14: 296–305

Nickel EH, Hallberg JA, Halligan R (1979) Unusual nickel mineralization at Nullagine, Western Australia. J Geol Soc Austral 26: 61–71

Novgorodova MJ (1983) Native metals in hydrothermal ores. Nauka Moscow, 287 p (in Russian)

Ohnenstetter M, Johan Z (in prep.) Silicate-glass inclusions in (Pt, Fe) alloys from the Durance river PGM association

Ramdohr P (1949) Über das Vorkommen von Heazlewoodit Ni_3S_2 and über ein neues ihn begleitendes Mineral: Shandit, $Ni_3Pb_2S_2$. Sitzber Deutsch Akad Wiss Berlin, Math Naturwiss Kl, Nr VI: 3–29

— (1980) The ore minerals and their intergrowths. 2nd edition, Intern Series Earth Sci 35. Pergamon Press, Oxford, 1205 p

Raub E, Plate W (1956) Tempering and decomposition of platinum–iridium alloys. Zeit Metallkunde 47: 688–693

Razin LV (1975) Minerals-natural alloys of gold from copper-nickel deposits of Norilsk. Trudy Min Muz Akad Nauk SSSR 24: 93–106 (in Russian)

— *Yurkina KV* (1971) Platinum-group minerals in ores of the Gusevogorsk titanomagnetite deposit (the Middle Urals). Geol Rudnych Mestorozh, 1971, No 2: 102–109 (in Russian)

Rudashevskii NS (1984) New model of differentiation of platinum-group elements in the lithosphere. Zap Vses Min Obsch 113: 521–539 (in Russian)

— *Menachikov YuN, Motchalov AG, Trubkin NV, Shumskaya NI, Zhdanov VV* (1985) Cuprorhodsite $CuRh_2S_4$ and cuproiridsite $CuIr_2S_4$, new natural thiospinels of platinum-group elements. Zap Vses Min Obsch 114: 187–195 (in Russian)

— *Zhdanov VV* (1983) Accessory platinum mineralization within a mafic-ultramafic intrusion in Kamchatka. Bull Mosk Obsch Izpyt Prirody otd geol 58: 49–59 (in Russian)

Schneider A, Esch U (1944) System copper–platinum. Z Electrochem 50: 290–301

Schwellnus JSI, Hiemstra SA, Gasparrini E (1976) The Merensky reef at the Atok Platinum mine and its environs. Econ Geol 71: 249–260

Shunk FA (1969) Constitution of binary alloys, 2nd supplement. McGraw-Hill Book Co, New-York, 720 p

Stockman HW, Hlava PF (1984) Platinum-group minerals in alpine chromitites from southwestern Oregon. Econ Geol 79: 491–508

Talkington RW, Watkinson DH, Whittaker PJ, Jones PC (1986) Platinum group elementbearing minerals and other solid inclusions in chromite of mafic and ultramafic complexes: chemical compositions and comparisons; in Metallogeny of basic and ultrabasic rocks (regional presentations), Theophrastus, Athens, pp 223–249

Tarkian M, Prichard HM (1987) Irarsite-hollingworthite solid-solution series and other associated Ru-, Os-, Ir-, and Rh-bearing PGM's from the Shetland ophiolite complex. Mineral Deposita 22: 178–184

Thalhammer OAR, Stumpfl EF (1988) Platinum-group minerals from Hochgrössen ultramafic massif, Styria: first reported occurrence of PGM in Austria. Trans Inst Min Metall sect B 97: 77–82

Toma SA, Murphy S (1978) Exsolution of gold from detrital platinum-group metal grains in the Witwatersrand auriferous conglomerates. Canad Mineral 16: 641–650

Voltchenko YuA, Netcheukhin VM, Radygin AI, Sandler GA (1975) New type of platinum mineralization in ultramafics of folded belts. Dokl Akad Nauk SSSR 224: 182–185 (in Russian)

Yu TH, Lin SJ, Chao P, Fang CS, Huang CS (1974) A preliminary study of some new minerals of the platinum group and another associated new one in platinum-bearing intrusions in a region of China. Acta Geol Sinica 2: 202–218 (in Chinese)

Zhdanov VV, Rudashevskii NS (1980) New type of Pt–Au mineralization in metasomatites after mafic rocks. Dokl Akad Nauk SSSR 252: 1452–1456 (in Russian)

Authors' addresses: Dr. *Z. Johan* and Dr. *M. Ohnenstetter*, GIS BRGM-CNRS, Centre de Recherches sur la Synthèse et la Chimie des Minéraux, 1A, rue de la Férollerie, 45071 Orléans, Cedex 2, France. Dr. *W. Fischer* and Dr. *J. Amossé*, Institut Dolomieu, rue Maurice Gignoux, 38031 Grenoble, Cedex, France.